Journal of Oceanography
Vol. 52, pp. 69 to 92. 1996

Detecting Fluctuations of the Kuroshio Axis South of Japan Using TOPEX/POSEIDON Altimeter Data

Shiro Imawaki[1], Mayumi Gotoh[2]*, Hiroyuki Yoritaka[3]**,
Noriya Yoshioka[4]** and Atsunobu Misumi[5]

[1]*Research Institute for Applied Mechanics, Kyushu University, Kasuga, Fukuoka 816, Japan*
[2]*Department of Earth System Science and Technology, Interdisciplinary Graduate School of Engineering Sciences, Kyushu University, Kasuga, Fukuoka 816, Japan*
[3]*Hydrographic Department, Maritime Safety Agency, 5-3-1 Tsukiji, Chuo-ku, Tokyo 104, Japan*
[4]*Kobe Marine Observatory, Japan Meteorological Agency, Nakayamate, Chuo-ku, Kobe 650, Japan*
[5]*Japan Marine Science and Technology Center, Natsushima, Yokosuka, Kanagawa 237, Japan*

(Received 6 January 1995; in revised form 4 August 1995; accepted 7 August 1995)

Sea surface dynamic topography (SSDT) can be divided into temporal mean SSDT and fluctuation SSDT. The former is approximated with a climatological mean SSDT and the latter is derived from satellite altimetry data, to give an approximated total SSDT (called a composite SSDT). The method is applied to detecting fluctuations of the Kuroshio axis south of Japan using TOPEX/POSEIDON altimeter data from the first year mission in 1992–1993. The fluctuation SSDT averaged over a wide area south of Japan clearly shows an annual cycle with an amplitude of about 15 cm. Temporal changes of SSDT along a subsatellite track crossing the Kuroshio compare moderately well with those estimated from repeated hydrographic observations, although there is a discrepancy of unknown origin. The composite SSDT also compares well with SSDT estimated from the same hydrographic data. Horizontal distribution of the surface geostrophic velocity component normal to subsatellite tracks is derived every ten days from the composite SSDT. Most locations of estimated strong eastward geostrophic velocities coincide well with locations of the Kuroshio axis determined every 15 days from *in situ* surface velocity measurements on various vessels; for example, a fairly large meander of the Kuroshio south of Honshu is clearly detected. It is concluded that the composite SSDT can be used reliably to detect fluctuations of the Kuroshio axis south of Japan.

1. Introduction

Using Seasat and Geosat data, satellite altimetry has been demonstrated to be very useful in detecting fluctuations of sea surface height and estimating fluctuations of surface geostrophic velocity (Fu, 1983; Douglas *et al*., 1987). A new altimetry satellite, TOPEX/POSEIDON (hereinafter abbreviated to T/P), was launched as a cooperative effort by the United States and France and has been observing the sea surface height since late September 1992 (Fu *et al*., 1994). Herein, we try to detect fluctuations of the Kuroshio axis south of Japan by the use of T/P altimeter data.

*Present affiliation: PASCO Environmental Science Institute, 2-32-1 Yoga, Setagaya-ku, Tokyo 158, Japan.
**Present affiliation: Japan Marine Science and Technology Center, Natsushima, Yokosuka, Kanagawa 237, Japan.

Sea surface height measured by a satellite altimeter consists of large-amplitude undulations of the geoid and small-amplitude undulations of sea surface dynamic topography. The sea surface dynamic topography, the departure of the sea surface from the geoid which results in oceanic near-surface pressure, is hereinafter abbreviated to SSDT; we have resisted the temptation to use the term "sea surface topography" and its abbreviation SST because SST is already widely used as the abbreviation for "sea surface *temperature*". We also avoid calling the departure "sea surface height" because, in marine geodesy, the term "sea surface height" includes the geoid undulations as well as the departure. The present geoid model is not accurate enough to extract satisfactorily the absolute SSDT from the sea surface height measured with altimeters, except for very large scale ocean circulation or for limited areas such as the western North Atlantic(Cheney and Marsh, 1981; Nerem *et al*., 1990; Imawaki *et al*., 1991).

The SSDT can be divided into two parts: the temporal mean SSDT and the deviation from it, or the fluctuation SSDT. The former is subject to the geoid inaccuracy, but the latter is free from that inaccuracy. Therefore, the temporal fluctuation SSDT can be determined as accurately as the measured sea surface height. The lost information on the temporal mean SSDT in the altimeter data processing must be provided in some independent way to estimate the absolute SSDT. A method used to solve this problem is to approximate the temporal mean SSDT with a climatological mean SSDT, such as geopotential anomalies at the sea surface calculated from historical hydrographic data. The sum of the climatological mean SSDT and fluctuation SSDT is herein called a composite SSDT, which is an approximation of the total SSDT. This method has been used successfully for the Gulf Stream and Kuroshio Extension regions (Willebrand *et al*., 1990; Imawaki and Ichikawa, 1991; Ichikawa and Imawaki, 1994). Another method used to solve the problem is to estimate the temporal mean SSDT associated with a strong jet from altimeter data alone. It has been successfully applied to some jets (Kelly and Gille, 1990; Tai, 1990; Qiu *et al*., 1991; Qiu, 1992, 1994), but requires the assumption that the location of the jet changes by an amount much greater than the width of the jet during satellite observations.

The Kuroshio changes its strength and axis location seasonally and inter-annually. For example, it is well known that the Kuroshio has more than one stable path south of Honshu and typically follows one path for several years before switching to another; Taft (1972) carefully studied two stable paths, one with and one without a large stationary meander, and Kawabe (1985) classified three typical paths including a nearshore non-large-meander path, offshore non-large-meander path and typical large-meander path (Fig. 1). In contrast, the location of the Kuroshio is known to be stable south of Shikoku, and therefore, the latter method mentioned above (e.g., Kelly and Gille, 1990) cannot be applied there. The present paper examines how well the composite SSDT, the former method, can detect actual fluctuations of the Kuroshio axis for the whole area south of Japan.

There are two major problems in using a composite SSDT, or approximating the actual mean SSDT with a climatological mean SSDT based on historical hydrographic data. One problem is that the climatological mean SSDT usually represents only the baroclinic field and ignores the barotropic field; here we define the barotropic component as the velocity at a chosen deep reference level. Namely, the velocity at the reference level such as 1,000 dbar surface is ignored because our knowledge of the deep mean flow is scant. On the other hand, an altimeter can measure the baroclinic plus barotropic field at the sea surface. Therefore, the composite SSDT is the sum of the baroclinic temporal mean field and the baroclinic plus barotropic temporal fluctuation field; it is lacking the barotropic temporal mean field. The other problem is the difference of observation periods. Altimeter observations continue at most for several years,

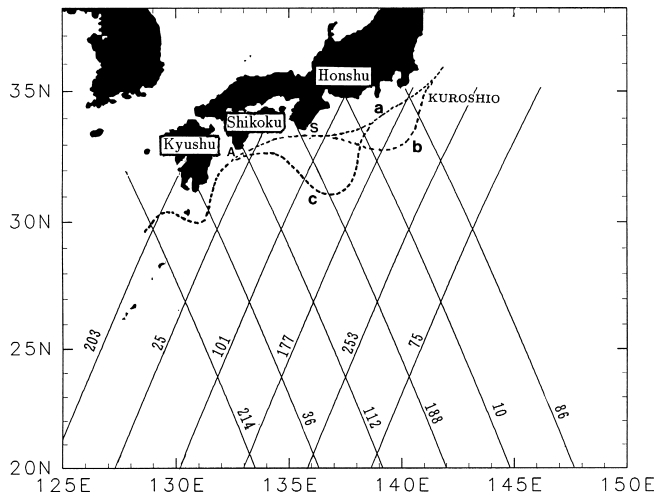

Fig. 1. T/P subsatellite tracks south of Japan, shown with Pass numbers. Superimposed broken lines are three typical paths of the Kuroshio at the sea surface (adapted from Kawabe, 1985): a for the nearshore non-large-meander path, b for the offshore non-large-meander path, and c for the typical large-meander path. Locations of two capes are shown: A for Cape Ashizuri, and S for Cape Shiono-misaki.

while historical hydrographic observations span several decades. Generally, the mean Kuroshio is broader and weaker when it is averaged over a longer period and where the current path is fluctuating more extensively. The difference of averaging periods between historical hydrographic observations and altimetric observations may cause a mismatch of the mean field. An extreme favorable case is that the Kuroshio is quite stable and the mean Kuroshio during the satellite mission is almost the same as the climatological mean Kuroshio. Another favorable case is that the Kuroshio path is fluctuating more extensively and frequently, and therefore, the mean Kuroshio is weaker there and the contribution of the associated mean SSDT to the composite SSDT is smaller than that of the fluctuation SSDT; the actual mean SSDT should not necessarily be approximated as accurately in this case.

There are plenty of studies on comparison of altimetric SSDT with tide gauge sea levels (e.g., Cheney *et al*., 1989; Mitchum, 1994). There are less number of studies, however, on comparison of horizontal profiles of altimetric SSDT with *in situ* SSDT profiles (Glenn *et al*., 1991; Horton *et al*., 1992) or comparison of geostrophic velocities derived from altimetric SSDT with *in situ* surface velocities (Picaut *et al*., 1990; Willebrand *et al*., 1990; Ebuchi and Hanawa, 1995; Ichikawa *et al*., 1995).

In this paper, we use T/P altimeter data for one year to detect the fluctuation component of SSDT for the Kuroshio region south of Japan (Fig. 1). First, temporal change of the spatial mean of fluctuation SSDT over a wider area (about 1,500 × 1,500 km) is analyzed to examine the uncertainty of the altimeter data. Then, the fluctuation SSDT is combined with a climatological mean SSDT to give a composite SSDT. The composite SSDT and geostrophic velocity derived from that are compared with several kinds of *in situ* data as follows. The composite SSDT along a subsatellite track is compared with the SSDT estimated from repeated hydrographic observations along the track. It is also compared with sea level data from a tide gauge station near the chosen track. The slope of the composite SSDT along subsatellite tracks is estimated to give the surface

geostrophic velocity component normal to the tracks. Horizontal distributions of the velocity component are compared with locations of the Kuroshio axis determined on the basis of *in situ* surface velocity measurements. The data and data processing used are described first, followed by the results of the comparison with hydrographic data and the determination of the variable Kuroshio axis location south of Japan. Finally, there are discussion and summary of these results.

2. Data and Data Processing

The satellite T/P began measuring sea surface height by microwave radar altimeters in late September 1992 (Fu *et al.*, 1994). The satellite takes exact repeat orbits over about a ten day period. Two altimeter systems are on board: the NASA (National Aeronautics and Space Administration) altimeter system, TOPEX, and the CNES (Centre National d'Etudes Spatiales) altimeter system, POSEIDON. We used data from both TOPEX and POSEIDON during the first 38 repeat cycles, or about one year from September 25, 1992 to October 3, 1993; the antenna is shared by the two altimeters and only one altimeter is measuring the sea surface height at any given time. The data were provided as TOPEX GDR (Geophysical Data Record) and Merged T/P Products by the Jet Propulsion Laboratory; those data sets are called GDR in this paper for convenience. We used data mostly from five descending passes and one ascending pass which cross typical paths of the Kuroshio south of Japan at almost right angles (Fig. 1). We also used the altimeter data from a wider area in the western North Pacific (between 20°N and the Japanese coast or 35°N) for examining the reliability of the data.

The altimeter data corrections used are as follows. Following the TOPEX GDR Handbook(Callahan, 1993) and AVISO User Handbook (AVISO, 1992), the altimeter data were extracted for subsatellite tracks south of Japan. The sampling interval is about one second, corresponding to 6.2 km along tracks. Three data quality flags provided in the GDR were used: the altimeter surface flag, TOPEX Microwave Radiometer surface flag and ocean tide flag. Using the standard GDR corrections, measured sea surface heights were corrected with electromagnetic bias correction, ionospheric correction, dry and wet tropospheric corrections, and inverse barometer correction. The uncertainty of altimeter distance measurements, including the above mentioned environmental corrections but excluding ocean tide correction, has been estimated to be about 3 cm in one-sigma value (Fu *et al.*, 1994). Ocean and solid earth tide corrections provided in the GDR are also applied; we used primarily the Cartwright and Ray (1991) tide model correction, with the Schwiderski (1980) model correction used for comparison. The ocean tide correction is considered to be the most serious problem in T/P altimeter data processing, but discussing the tidal correction in detail is beyond the scope of this paper. No correction was made for the satellite radial orbit error because its estimated error is small (about 4 cm) for T/P (Fu *et al.*, 1994). There is a relative bias between the TOPEX and POSEIDON altimeter systems and 20 cm bias was applied here tentatively. This altimeter bias depends on electromagnetic bias correction algorithms used, among others, and should be revised later because the electromagnetic bias algorithms presently used have been found inaccurate (Gaspar *et al.*, 1994). See Fu *et al.* (1994) for more details.

The data processing to obtain the fluctuation SSDT is as follows; in principle, we used the so-called collinear method (Cheney *et al.*, 1983). The mean sea surface height (including geoid undulations and the mean SSDT) provided in the GDR was subtracted from the sea surface height corrected above in order to reduce apparent fluctuations of SSDT caused by the combined effect of lateral fluctuations of subsatellite tracks and the geoid undulations (Callahan, 1993); those apparent fluctuations are not negligible where geoid undulation is steep even if the fluctuations

of subsatellite tracks are controlled within ±1 km at the equator. After the data were carefully examined visually to locate and exclude doubtful data (less than 1%), they were interpolated to fixed nominal points along tracks, and then means over the entire measurement period (one year) were calculated at those points; here the nominal points were chosen to be the data points during the second repeat cycle of T/P mission. Finally, the deviation from the mean was calculated at each nominal point and for each cycle. This is the fluctuation SSDT that we want to estimate. The fluctuation SSDT data were smoothed along the tracks by a three-point symmetric low-pass filter which has weights of 1/4, 1/2 and 1/4, and the half power gain at a wavelength of about 30 km.

The altimeter cannot measure the sea surface height very close to the coast, especially when the satellite flies from land to sea such as for the five descending passes in the present case. To utilize the altimeter data as close to the coast as possible, we re-examined the data near coastal ends along Passes 36, 112, 188 and 86, and recovered subjectively about 50% of original data for which the TOPEX Microwave Radiometer may not provide us with accurate wet tropospheric correction. We also used unfiltered data of the SSDT near the coastal ends. These exceptional data processing procedures have improved the results considerably.

The climatological mean SSDT was derived from geopotential anomalies at the sea surface referred to 1,000 dbar surface with approximated conversion of 1 dynamic m (10 m^2/sec^2) to 1 m in linear scale. The anomalies were calculated for $1° \times 1°$ boxes from historical hydrographic data collected and compiled since 1907 by the Japan Oceanographic Data Center. The standard deviation of those anomalies is typically 20 cm in the Kuroshio region south of Japan, except for the stationary meander region, where it reaches up to 50 cm at 32°N, 138°E. Note that this standard deviation includes a possible annual cycle of SSDT. Choosing the reference level is a compromise between the desired deeper levels and a reduced number of observations at deeper layers. Our best choice was the 1,000 dbar surface, which is deep enough to be used as a reference level to approximate the surface topography of the Kuroshio. The mean SSDT along subsatellite tracks was estimated by linear interpolation from this data set.

The geostrophic velocity component normal to subsatellite tracks was estimated from the gradient of the composite SSDT, i.e., the sum of the climatological mean SSDT and fluctuation SSDT. The estimated geostrophic velocities were smoothed by running averages over four data-points along tracks to reduce the measurement noise. This low-pass filter has the half power gain at a wavelength of about 50 km. The uncertainty of the T/P altimeter measurements is estimated to be about 3 cm (Fu *et al*., 1994), except for errors having large horizontal scales, whose contribution to the local gradient of SSDT is small; these errors include orbit and tidal correction errors and large-scale intraseasonal fluctuations of unknown origin discussed below. Therefore, the uncertainty of the temporal fluctuation part of those geostrophic velocities is estimated to be 0.1–0.2 m/sec. Note, however, that the uncertainty of the temporal mean part of the geostrophic velocities is unclear because it includes the effect of approximating the one year mean SSDT with the climatological mean SSDT.

Hydrographic observations were carried out repeatedly along a T/P subsatellite track (Pass 112) crossing the Kuroshio south of Japan to obtain sea surface geopotential anomalies referred to 1,000 dbar surface for comparison with altimetric SSDT. Dates of these observations are listed in Table 1. Each ship listed in the table was equipped with a Neil Brown Mark III B conductivity-temperature-depth recorder (CTD). The pressure, temperature and salinity uncertainty of the calibrated CTD data are believed to be ±3 dbar, 0.005°C and 0.01 psu, respectively. The uncertainty of estimated geopotential anomalies due to those uncertainties is small (within 1 dynamic cm). The actual hydrographic data, however, include fluctuations of small scales in time

Table 1. Comparison of the composite SSDT with the hydrographic SSDT along T/P Pass 112 (Fig. 5). Ship names and dates of hydrographic surveys are shown together with altimeter cycles from which the composite SSDT is interpolated at the time of the hydrographic measurements. The rms difference between the altimetric and hydrographic SSDT's is shown in cm.

Case	Hydrographic survey	Cycles	Difference
I	Shoyo; Nov. 28–30, 1992	7, 8	14
II	Shumpu-maru; May 30–31, 1993	25, 26	22
III	Kaiyo; July 2–5, 1993	29, 30	8
III′	Shoyo; July 6–7, 1993	29, 30	7
IV	Shumpu-maru; July 31, 1993	32	8
V	Shumpu-maru; Sept. 25–26, 1993	37, 38	12

and space (such as internal tides and small scale fluctuations of the Kuroshio) which cannot be resolved by those discrete measurements. Therefore, the uncertainty of the geopotential anomalies may be up to 10 dynamic cm when horizontal profiles based on hydrographic observations carried out during several days are concerned. At a station on the continental slope shallower than 1,000 m, geopotential anomalies referred to 1,000 dbar cannot be estimated but equivalent geopotential anomalies can be estimated as follows; the difference of sea surface geopotential anomaly referred to the common deepest level between that station and the next offshore station is subtracted from the sea surface geopotential anomaly referred to 1,000 dbar surface (or the equivalent one) at that offshore station, which assumes that there is no motion at that common deepest level near the bottom (instead of the 1,000 dbar level). The CTD observations made by the R/V Shumpu-maru were supplemented by observations with a Tsurumi-Seiki expendable bathythermograph (XBT) for the May and July surveys in 1993 and by observations with a Tsurumi-Seiki digital bathythermograph (DBT) for the September survey; the uncertainty of these temperature data is estimated to be about 0.1°C. To calculate geopotential anomalies from XBT or DBT temperature profiles, salinities were determined by averaging salinity profiles at the two neighboring CTD stations, and temperatures below the 460 m (for XBT) or 750 m (for DBT) depth were determined similarly, which introduces additional uncertainty of geopotential anomalies of 2–3 dynamic cm (Takano *et al.*, 1981). The geopotential anomalies in dynamic m are converted to the SSDT in m of linear scale in the remainder.

To compare horizontal distribution of estimated geostrophic velocities with *in situ* data, we use locations of the Kuroshio axis shown in reports issued twice a month by the Hydrographic Department, Maritime Safety Agency, Japan and entitled "Prompt Report on Oceanographic Conditions" (hereinafter abbreviated to Prompt Report). The surface Kuroshio map for the first half of June 1993 shown in the Prompt Report is reproduced in Fig. 2 as an example. Axis locations in the Prompt Report have been determined mainly from surface layer velocities (at 10–20 m depth) measured by acoustic Doppler current meters on various vessels. Temperatures at 200 m depth (or 100 m depth in some cases) have been used supplementarily as an indicator of the Kuroshio axis following previous analyses (Kawai, 1969). When determining the location, the width of the Kuroshio has been fixed to 65 km and the location of the axis (the strongest part of the Kuroshio) is assumed to be located at one third of this Kuroshio width from the shore-side edge of the Kuroshio, following the statistical analysis of Masuzawa (1969); note that the horizontal shear of the surface Kuroshio is larger on the shore-side than on the offshore-side. The

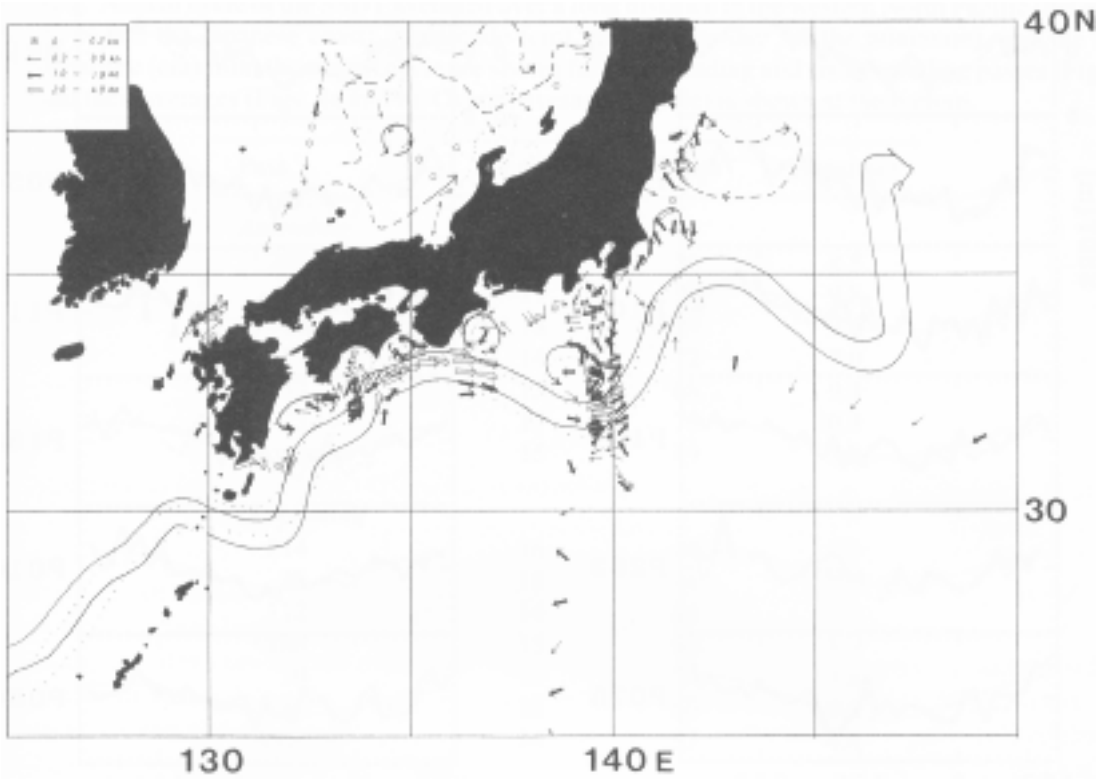

Fig. 2. Location of the Kuroshio axis south of Japan for the first half of June 1993, determined from *in situ* surface velocity data (reproduced from "Prompt Report on Oceanographic Conditions").

uncertainty of the Kuroshio axis thus determined is believed to be about 20 km. Locations of the Kuroshio axis were read from Prompt Report maps with resolution of about 10 km.

Sea level data obtained at a float-type tide gauge station (32°46′ 33″ N, 132°57′ 41″ E) at Tosashimizu on Cape Ashizuri (Fig. 1) are used for comparison with the altimeter data. Daily mean sea levels at dates of hydrographic measurements are used after inverse barometer correction. The sea level data at this coastal station were not comprehensively compared with the altimetry data, because sea level data from coastal stations have been shown to compare worse with the altimetry data than those from island stations (Mitchum, 1994; Ichikawa and Imawaki, 1996).

3. Results

3.1 Uncertainty of altimeter data

Before looking at the T/P altimeter data for the Kuroshio region, we examine the uncertainty of the altimeter data after all corrections were made. Time series of the fluctuation SSDT averaged over a long distance in the western North Pacific are shown in Fig. 3. This area is located in the western-most part of the North Pacific subtropical gyre, where sea surface geopotential anomalies are the highest in the gyre (Wyrtki, 1975). Most of the area is located in the Philippine

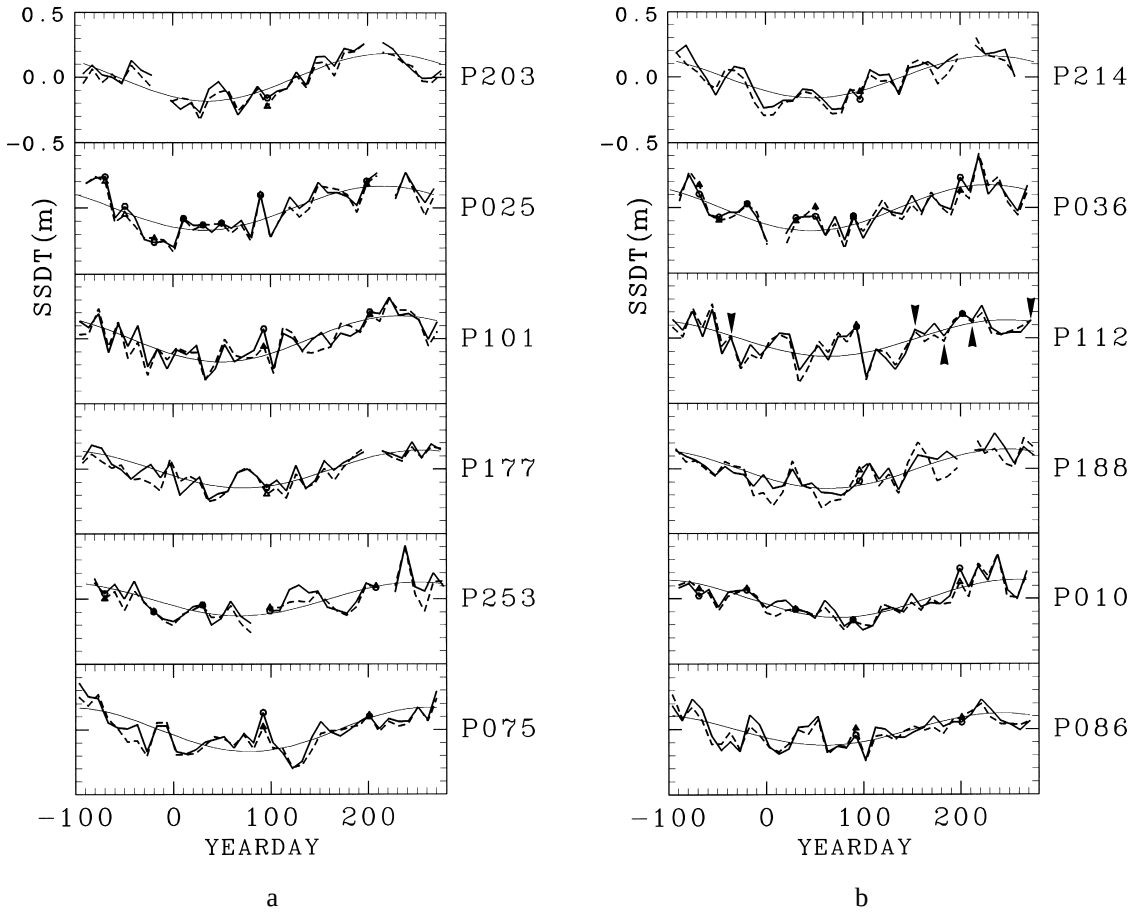

Fig. 3. Time series of the fluctuation SSDT averaged over a long distance in the western North Pacific (between 20°N and the Japanese coast) along (a) six ascending and (b) six descending passes. Abscissa is the year-day of 1993. Results for the Cartwright and Ray (1991) tide model correction (solid lines) and those for the Schwiderski (1980) model correction (broken lines) are shown. Circles and triangles indicate POSEIDON measurements. Annual sinusoidal curves fitted to the Cartwright and Ray (1991) model results are shown by thin solid lines. Pass numbers are shown on the right-hand side. Arrows for Pass 112 indicate cycles for which the comparison shown in Fig. 5 is made.

Basin, which is separated from the North Pacific Basin by the Izu-Ogasawara Ridge located at 140°–145°E longitudes. As is shown below, three kinds of fluctuations are apparent: an annual fluctuation, intraseasonal fluctuation and an about 30 day period fluctuation.

Fluctuations over about a one year period are apparent in each pass. The annual sinusoidal curve is fitted to the data corrected by the Cartwright and Ray (1991) tide model (Fig. 3 and Table 2). The amplitude of the fitted curve is 16 ± 2 cm on average for six ascending passes and 15 ± 2 cm for six descending passes; here, the standard deviation is given as well as the average. The phase (year-day for the minimum) is day 56 ± 18 (February 25) on average for ascending passes, and day 60 ± 10 (March 1) for descending passes. The amplitude and phase of the annual sinusoidal curve fitted to the data corrected by the Schwiderski (1980) tide model are almost

Table 2. Annual cycle of the SSDT averaged over a long distance in the western North Pacific (between 20°N and the Japanese coast). Amplitude (cm), phase (year-day for the minimum), and the rms departure (cm) from the annual cycle are shown for six ascending and six descending passes (Fig. 3) and their averages (Figs. 4a and b). Overall average (Fig. 4c) is shown at the bottom.

Pass	Amplitude	Phase	Departure
Ascending			
203	18	36	8.5
25	17	32	9.8
101	18	49	9.4
177	14	72	7.0
253	13	68	9.3
75	17	78	10.3
Average	15	49	3.9
Descending			
214	16	49	7.9
36	18	46	9.2
112	14	64	10.4
188	15	64	6.4
10	15	74	7.8
86	12	60	9.6
Average	14	57	4.8
Overall average			
—	15	53	4.0

identical with these values. Figures 4a, b and c show fluctuations averaged over all ascending passes, all descending passes and all passes, respectively. The amplitude and phase are shown in Table 2. The annual cycle is apparent; the overall average shows the amplitude of 15 cm and the phase of year-day 53 (February 22), which are almost identical with averages of amplitudes and phases for the individual passes mentioned above. These results are quite consistent with the observed annual cycle of sea surface geopotential anomaly referred to 1,000 dbar at 29°N, 135°E in this area; its climatological mean amplitude estimated from monthly data is 13 dynamic cm and the minimum occurs in March (Wyrtki, 1975).

Also apparent in Fig. 3 are intraseasonal fluctuations of a several ten days period. The rms departure from the annual cycle is 9 ± 1 cm on average both for ascending and descending passes. Those fluctuations are not correlated with each other between neighboring passes, with correlation coefficients (ranging from –0.13 to 0.28) far below the 95% significance level. This means that the SSDT, averaged over about 1,500 km along subsatellite tracks, fluctuates independently with the SSDT on the neighboring tracks separated only by about 250 km, which can hardly be considered to be a real oceanic phenomenon. Most of these fluctuations relative to the annual cycle are thought to be measurement noise. A small fraction of the fluctuations comes from the fluctuation of the Kuroshio axis location mentioned below, but this effect can be found negligibly small, considering that the ratio of the Kuroshio location shift to the horizontal extent of the present averaging is small.

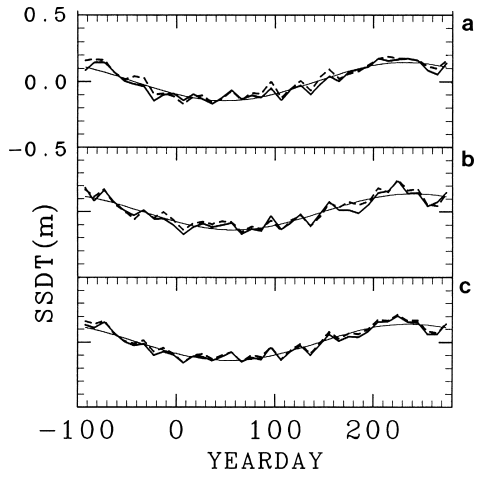

Fig. 4. The same as Fig. 3 except for averages for (a) ascending, (b) descending and (c) all passes.

Most of those fluctuations may be measurement noise, but part of fluctuations may reflect the real oceanic signal as shown below. When the fluctuations are averaged over all ascending and descending passes (Figs. 4a and b), most of departures from the annual cycle are canceled out resulting in the small rms departure (3.9 and 4.8 cm for ascending and descending, respectively), which indicates that the fluctuations are almost random among passes as mentioned above. An interesting point is that the fluctuations averaged for ascending and descending passes are quite similar to each other, with similar rms departure (3.9 and 4.8 cm) and a high correlation coefficient of 0.61 which is far above the 95% confidence level. The fluctuation averaged for all the passes (Fig. 4c and Table 2) has an rms departure from the annual cycle of 4.0 cm, larger than the estimated uncertainty of 2.5 cm, which assumes that the fluctuations for 12 individual passes having an average rms departure of 9 cm are random. The results suggest that the sea level over this whole area (about 1,500 km × 1,500 km) fluctuates with an amplitude of about 4 cm and a dominant period of about 30 days (the total length of the observation period divided by 14 peaks found in Fig. 4c). The fluctuations might be related with velocity fluctuations with about a 30 days period which have been observed by moored current meters in this area of the Philippine Basin (Taira and Teramoto, 1981; Fukasawa and Teramoto, 1986; Takematsu *et al.*, 1986). The present data set, however, is too coarse in temporal resolution (ten days) to discuss such high-frequency fluctuations in detail. If this fluctuation (4 cm amplitude) is considered to be the real oceanic signal, the uncertainty of the altimeter data is reduced from 9 cm mentioned above to 8 cm. Note that this uncertainty has a large horizontal scale (longer than 1,500 km), so its effect is almost negligible in the later geostrophic calculation.

3.2 Comparison with hydrographic data

The composite SSDT along T/P Pass 112 is compared with the SSDT estimated from hydrographic data for six cases. Here, the composite SSDT is linearly interpolated at the time of the hydrographic observations. Figure 5 and Table 1 show the results. As shown in the previous section, the uncertainty of the SSDT estimated from the hydrographic data may be up to 10 cm. Except for case II, the comparison is fairly good; especially for case IV, an unusually high sea level (20–30 cm) is observed in both SSDT's quite consistently. The comparison is not so good,

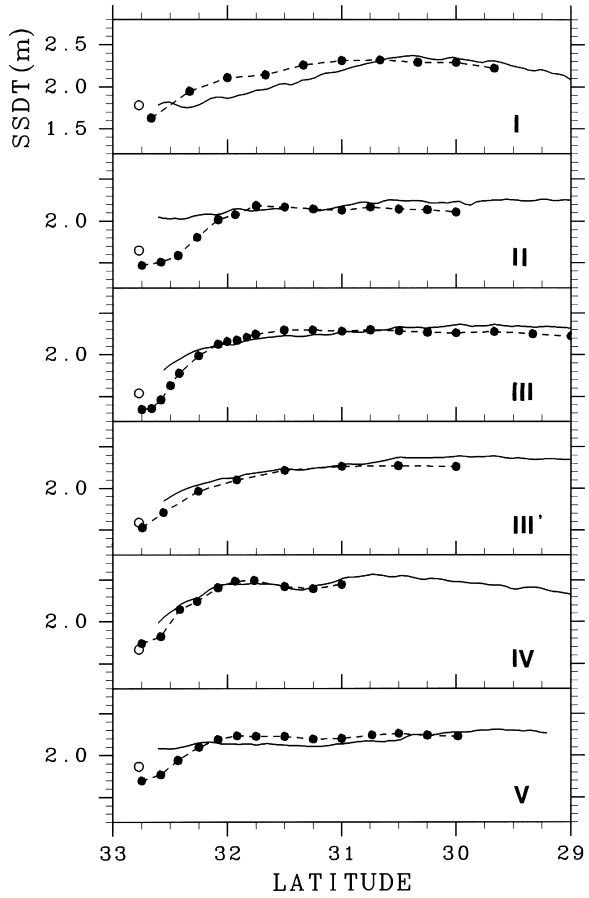

Fig. 5. Comparison of the composite SSDT (solid lines) from TOPEX altimeter data with the hydrographic SSDT (broken lines with dots) and daily mean sea levels at the tide gauge station (circles) for Pass 112. The composite SSDT is interpolated at the time of hydrographic observations. Case numbers (Table 1) are shown at the lower right corner of each panel. Note that the reference coordinate of the tide gauge data is different from that of the other two.

however, for case II, for which the rms difference (22 cm) is large and some remarkable discrepancy is found near the strongest part of the Kuroshio (north of 32°10′ N).

The interpolated composite SSDT and hydrographic SSDT are also compared with the daily mean sea level data at Tosashimizu near the coastal end of the pass (Fig. 5). Note that the reference coordinate of the tide gauge data is different from that of the present SSDT. The difference between the tide gauge sea level and the composite SSDT near the coastal end is almost constant (22–40 cm), except for case I (0 cm). The difference between the tide gauge sea level and the hydrographic SSDT at the coastal end is also almost constant (–6 to –19 cm), except for case IV (7 cm).

Figure 6 and Table 3 show the comparison of temporal changes of the SSDT along Pass 112 between the altimetric and hydrographic measurements, based on the same data shown in Fig. 5; this comparison is free from the issue of replacement of the one year mean SSDT with the climatological mean SSDT in order to calculate the composite SSDT, while the comparison of

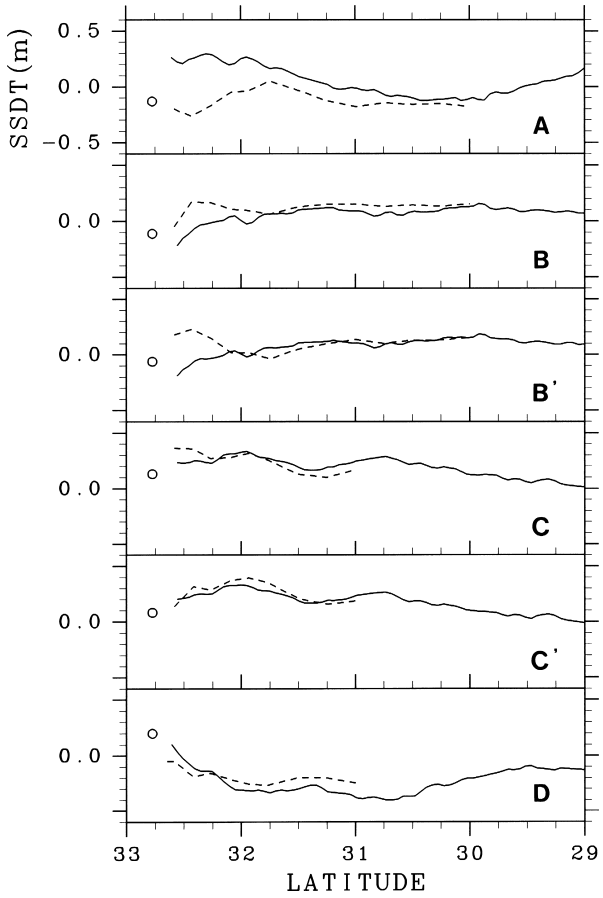

Fig. 6. Comparison of temporal changes of the SSDT along Pass 112 detected by TOPEX altimeter data (solid lines) with those estimated from hydrographic data (broken lines) and those from tide gauge data (circles). Case numbers (Table 3) are shown at the lower right corner of each panel.

the composite SSDT (Fig. 5) is subject to it. The difference between the altimetric and hydrographic measurements is small for cases C and C′ (in Table 3) and for case D, the rms difference being smaller than the uncertainty. The unusually high sea level for case IV is shown again clearly for both the altimetric and hydrographic SSDT's; a large positive change for cases C and C′ , and a large negative change for case D having similar amplitude (20–30 cm) are observed by the two measurements consistently. A rather large discrepancy (30–40 cm) is found, however, north of 32°N for case A, and for cases B and B′ , which is mostly related with the discrepancy found in comparison of the composite SSDT for case II shown above (Fig. 5). Also shown in Fig. 6 are time changes of the tide gauge sea levels, which can be directly compared with the changes of the altimetric SSDT because the comparison is free both from the reference coordinate issue and the barotropic/baroclinic issue described in the Introduction. The temporal changes of these two are fairly similar to each other except for case A.

3.3 Surface geostrophic velocity

Figure 7 shows time series of horizontal distribution of the surface geostrophic velocity

Table 3. Comparison of temporal change between the altimetric and hydrographic SSDT's along Pass 112 (Fig. 6). See Table 1 for observation numbers. The rms difference is shown in cm.

Case	Obs. No.	Difference
A	I, II	25
B	II, III	11
B′	II, III′	11
C	III, IV	6
C′	III′, IV	6
D	IV, V	9

component normal to subsatellite tracks in the Kuroshio region south of Japan. The velocities are estimated from the gradient of the composite SSDT obtained every ten days, and filtered to reduce fluctuations of horizontal wave-length shorter than 50 km. Horizontal bars represent locations of the Kuroshio axis shown in the Prompt Report issued every 15 days. For each cycle, the nearest Prompt Report was chosen to indicate the location of the Kuroshio axis, resulting in a nominal maximum time lag between the two measurements of eight days and a possible maximum time lag of 15 days. As is noted in the previous section, the uncertainty of these locations of the Kuroshio axis in the Prompt Report is about 20 km. Note that the determined locations of the Kuroshio axis are averages over 15 days, in principle, while the estimated distribution of geostrophic velocity is instantaneous. Also note that wide widths of the Kuroshio, for example, those seen during Cycles 5 and 6 for Pass 86 (Fig. 7f), mean that the Kuroshio was flowing almost parallel to or meandering around that subsatellite track during those particular cycles.

Locations of estimated strong eastward geostrophic velocities generally coincide well with locations of the Kuroshio axis shown in the Prompt Report considering that the two data sets do not represent simultaneous measurements. The comparison is very good, in particular, for Passes 36, 10 and 86 (Figs 7b, e and f), where the location of the Kuroshio axis changes extensively. The Prompt Report shows that the Kuroshio abruptly took a fairly large (but not stationary) meander path south of Honshu in early April 1993 (corresponding to Cycle 21) and that the pattern continued until September 1993, although the amplitude of meander shrank gradually. This change of the Kuroshio path is clearly seen in the change of the estimated eastward geostrophic velocities from Cycles 19 to 21 for Pass 10 (Fig. 7e). The estimated surface geostrophic velocities of the Kuroshio during the meander are large, ranging from 1.5 to 2.5 m/sec, although those are probably overestimate (10–20%) because the effect of centrifugal force is not taken into account; the Prompt Report also shows strong surface velocities along the meander path, especially on Pass 10, for which the report indicates the maximum speed range class, 2–5 knots (1.0–2.5 m/sec). Fairly strong westward surface geostrophic flows (about 0.5 m/sec) are estimated in the recirculation area north of the meandering Kuroshio during Cycles 21 through 38, which is in accord with descriptions shown in the Prompt Report. Those flows are associated with the presence of the large cyclonic cold water mass located on the shore-side of the meandering Kuroshio.

The comparison is fairly good for Passes 112 (off Cape Ashizuri; Fig. 7c) and 188 (off Cape Shiono-misaki; Fig. 7d). Locations of estimated strong eastward geostrophic velocities coincide well with locations of the Kuroshio reported by the Prompt Report when the Kuroshio path was

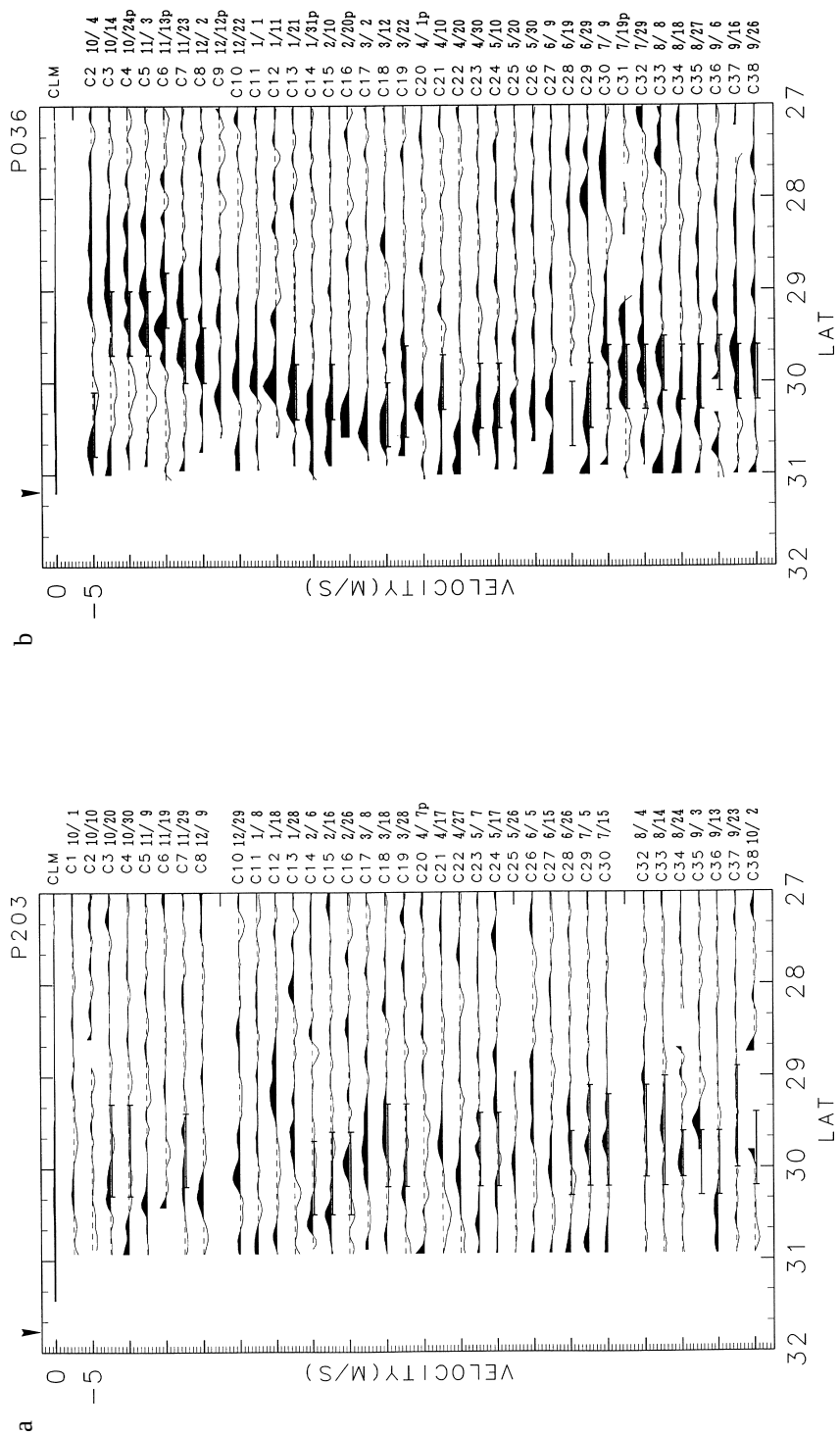
a
P203
CLM
C1 10/ 1
C2 10/10
C3 10/20
C4 10/30
C5 11/ 9
C6 11/19
C7 11/29
C8 12/ 9
C10 12/29
C11 1/ 8
C12 1/18
C13 1/28
C14 2/ 6
C15 2/16
C16 2/26
C17 3/ 8
C18 3/18
C19 3/28
C20 4/ 7p
C21 4/17
C22 4/27
C23 5/ 7
C24 5/17
C25 5/26
C26 6/ 5
C27 6/15
C28 6/26
C29 7/ 5
C30 7/15
C32 8/ 4
C33 8/14
C34 8/24
C35 9/ 3
C36 9/13
C37 9/23
C38 10/ 2
0
-5
VELOCITY(M/S)
32
31
30
29
28
27
LAT
b
P036
CLM
C2 10/ 4
C3 10/14
C4 10/24p
C5 11/ 3
C6 11/13p
C7 11/23
C8 12/ 2
C9 12/12p
C10 12/22
C11 1/ 1
C12 1/11
C13 1/21
C14 1/31p
C15 2/10
C16 2/20p
C17 3/ 2
C18 3/12
C19 3/22
C20 4/ 1p
C21 4/10
C22 4/20
C23 4/30
C24 5/10
C25 5/20
C26 5/30
C27 6/ 9
C28 6/19
C29 6/29
C30 7/ 9
C31 7/19p
C32 7/29
C33 8/ 8
C34 8/18
C35 8/27
C36 9/ 6
C37 9/16
C38 9/26
0
-5
VELOCITY(M/S)
32
31
30
29
28
27
LAT

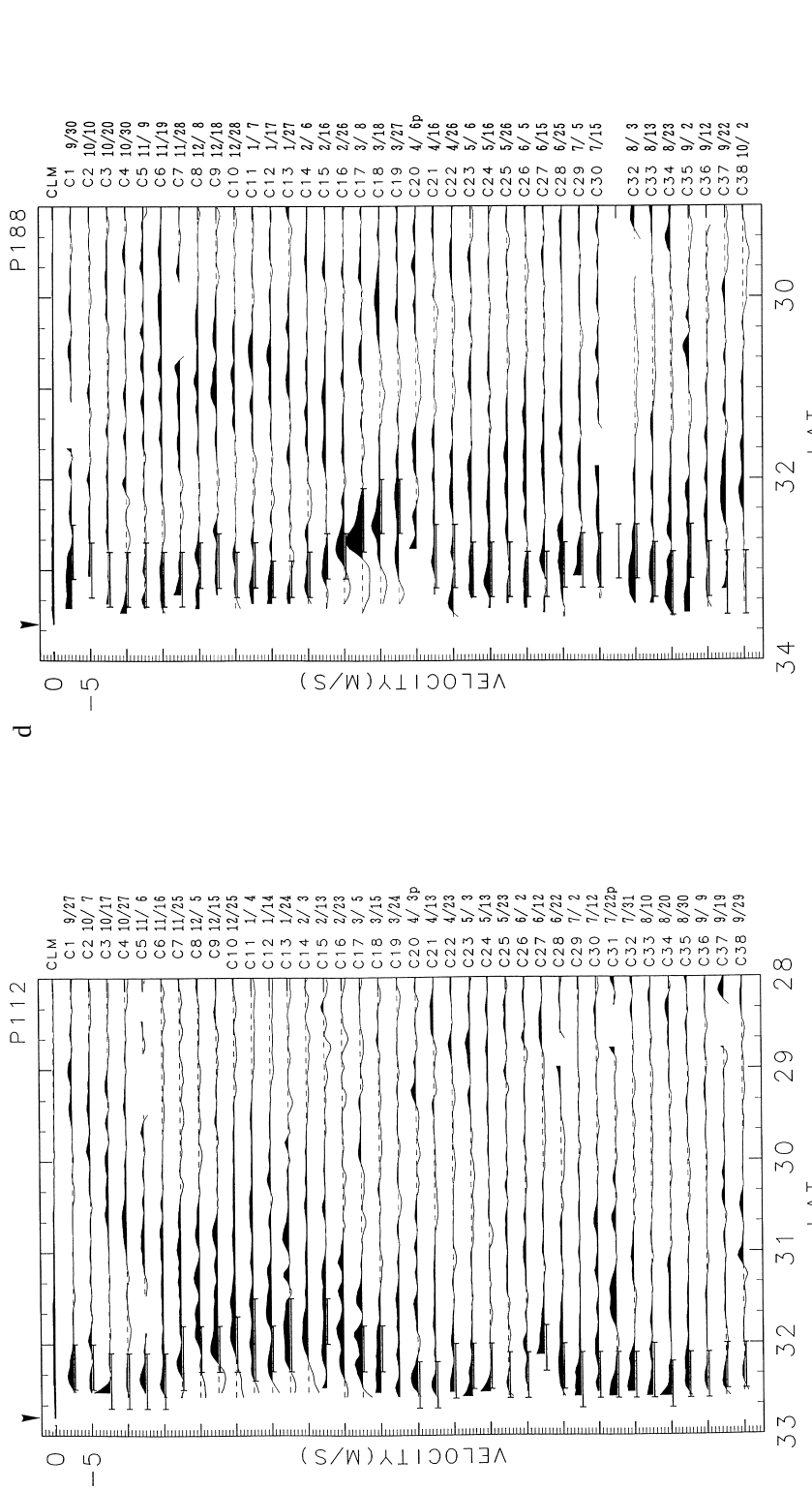

Fig. 7. Time series of horizontal distribution of the surface geostrophic velocity component normal to subsatellite tracks in the Kuroshio region south of Japan from late September 1992 to early October 1993; (a) is for Pass 203, (b) for 36, (c) for 112, (d) for 188, (e) for 10, and (f) for 86. At the top of each panel is shown the distribution of surface geostrophic velocity (labeled "CLM") estimated from the climatological mean SSDT. Numbers of ten day repeat cycles and measurement dates are shown on the right-hand side with the label "p" indicating POSEIDON measurements. Positive (dark shading) represents eastward flow. The velocity scale is shown at the upper left corner. Each distribution is drawn with 2.5 m/sec offset. Zero velocity is shown as a dashed line. Horizontal bars show locations of the Kuroshio axis determined from *in situ* surface velocity measurements and reported in "Prompt Report on Oceanographic Conditions". An arrow shows the location of the coast.

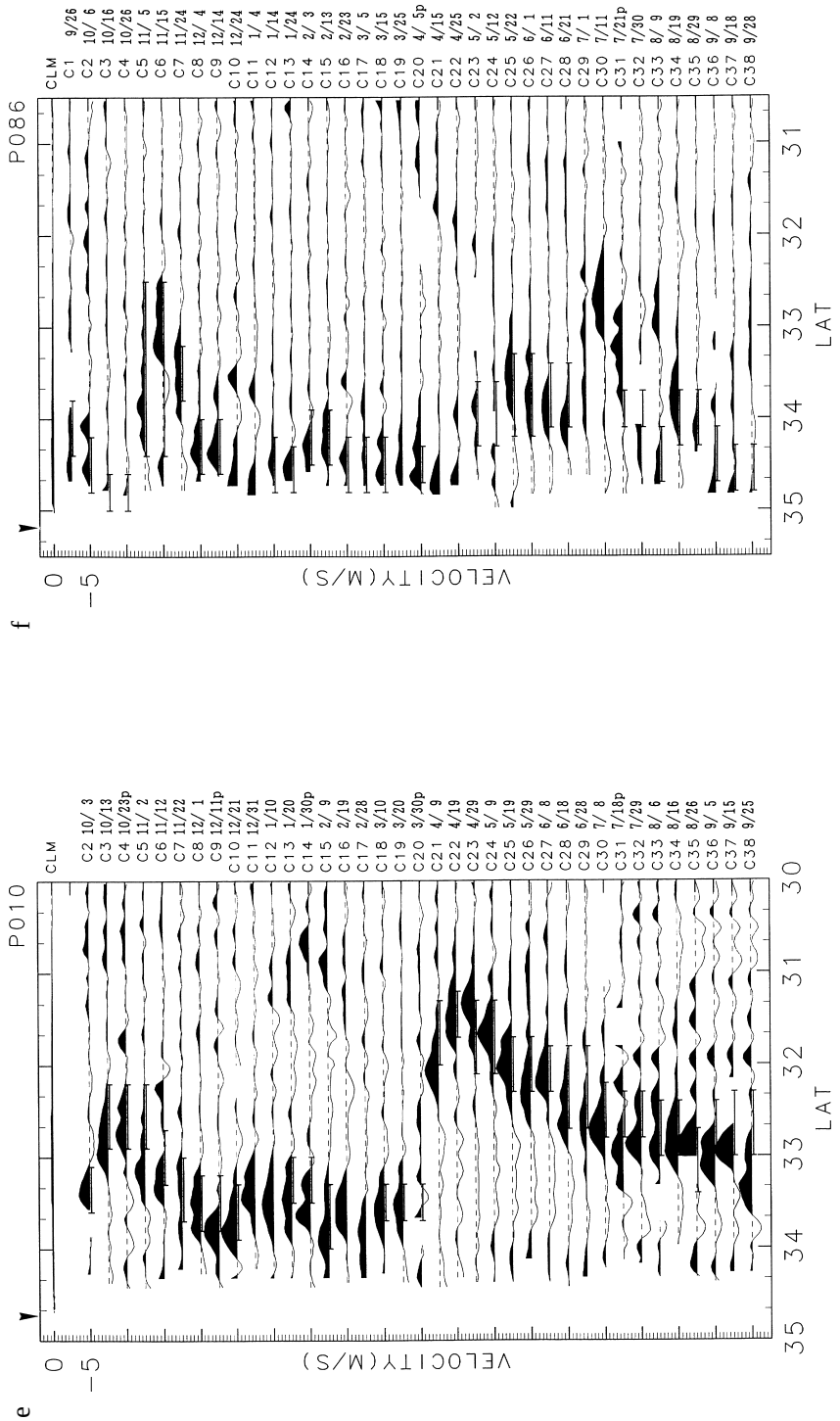

Fig. 7. (continued).

located offshore. When the Kuroshio was flowing near the coast, a considerable part of the flow is detected by the estimated geostrophic velocities but some part seems to be missing, for example, for Pass 112 during Cycles 4, 25 and 38, and for Pass 188 during Cycles 2–5, 9–10, 25 and 36–38.

The comparison is not good for Pass 203 (Fig. 7a); several locations of estimated strong eastward velocities agree well with locations of the reported Kuroshio path, but sometimes no strong eastward velocities were found where the Kuroshio path was reported, for example, during Cycles 4, 24, 32 and 37. The composite SSDT was not obtained north of 31°N because of lack of tidal correction.

Table 4 shows the results of this comparison statistically. Locations of the maximum estimated geostrophic velocity are compared with locations of the Kuroshio axis determined from *in situ* surface velocity data. Except for Pass 203, the comparison is fairly good; bias of the difference of these locations is small (10–15 km), and the rms difference is also small (about 30 km) considering the uncertainty (about 20 km) of the Kuroshio axis determination and the time difference (up to 8–15 days) between the two measurements. Correlation coefficients between the two locations are significantly different from zero at the 95% confidence level for all passes. They are far above that confidence level especially where the rms location fluctuation is large, such as for Passes 36, 10 and 86. An interesting point is that the rms location fluctuation is, in general, larger for geostrophic velocity than for *in situ* velocity. This is partly because distribution of the geostrophic velocity is determined from instantaneous measurements, while locations of the Kuroshio axis determined from *in situ* velocity are, in principle, averages for 15 days.

It is interesting to trace the origin of the fairly large meander of the Kuroshio south of Honshu observed on Pass 10 during Cycles 21 through 38 (Fig. 7e). A slight offshore meander found on Pass 188 during Cycles 15 through 19 is surely its precursor (Fig. 7d). This small disturbance is further traced back to the meander of the Kuroshio southeast of Kyushu found on Pass 36, which was shifted steadily from offshore (29°N in Cycle 3) to the coast (30°N in Cycle 13). This is actually a reflection of a slow northeastward propagation of a Kuroshio meander which is clearly seen in a similar plot for ascending Pass 25 (Fig. 8), where locations of a pair of strong eastward and westward geostrophic velocities are shown to move quite steadily from south (the maximum eastward velocity at 29°N and westward on 30°N, in Cycle 3) to north (eastward at 31° 30′ N and

Table 4. Statistical comparison of locations of the maximum estimated geostrophic velocity with locations of the Kuroshio axis determined from *in situ* surface velocity data. Bias and rms difference are shown in km. Positive difference means that the maximum geostrophic velocity is located offshore compared with the Kuroshio axis. Also shown are the rms location fluctuation (km) (F_G for geostrophic velocity and F_I for *in situ* velocity) and their correlation coefficient (*C.C.*).

Pass	No. of data	Bias	Difference	F_G	F_I	*C.C.*
203	18	–11	39	45	19	0.50
36	21	3	30	54	33	0.88
112	28	13	30	39	24	0.63
188	28	10	28	38	25	0.47
10	32	–13	28	79	76	0.92
86	25	19	33	52	39	0.80

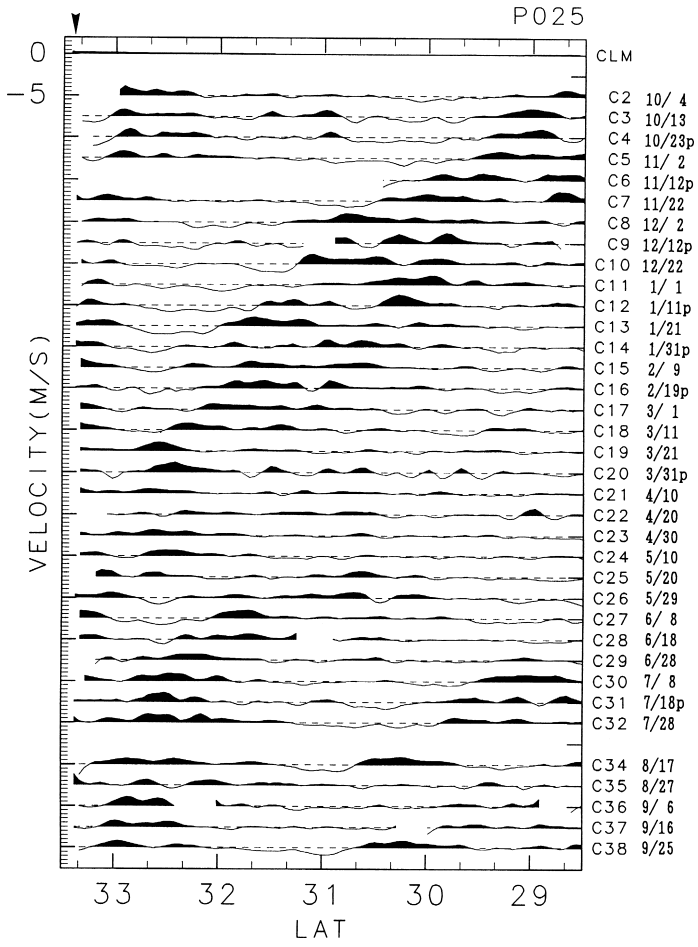

Fig. 8. The same as Fig. 7 except for Pass 25.

westward on 32° 30′ N, in Cycle 13) with an average meridional phase speed of about 3 cm/sec. Namely, a meander of the Kuroshio originally located southeast of Kyushu moved to northeast along the Japanese coast and finally became a fairly large meander south of Honshu. The propagation is also observed in Prompt Report since late October 1992.

4. Discussion

In the previous section, it is shown that the composite SSDT, derived from altimeter data combined with the climatological mean SSDT, can detect fluctuation of the Kuroshio axis well. For example, a fairly large meander of the Kuroshio south of Honshu is clearly detected in a time series of estimated surface geostrophic velocities on Pass 10 (Fig. 7e). The associated recirculation in the shore-side cold water region is also observed in the time series. The origin of this disturbance is traced to the meander located southeast of Kyushu in Cycle 3, which moved along the Japanese coast. This eastward propagation of the meander of the Kuroshio is contrary to the general tendency of the westward propagation of meanders of the Kuroshio Extension (Ichikawa and Imawaki, 1994; Aoki *et al.*, 1995).

Time series of the fluctuation SSDT (Figs. 3 and 4) averaged over a wide area in the western North Pacific (mostly in the Philippine Basin) clearly show an annual cycle of the SSDT, which is probably due to the heating and cooling of the surface layer above the seasonal thermocline. These time series also show large-scale (longer than 1,500 km) intraseasonal fluctuations with an average amplitude of 9 cm. Part of the fluctuation may be due to the real sea level rising and falling over the whole area with an amplitude of 4 cm and a dominant period of about 30 days. The reminder of the 8 cm rms fluctuation is thought to be measurement noise; in part it is probably due to the orbit error which is expected to be about 4 cm (Fu *et al*., 1994), but the sources of the remaining error of 7 cm as a one-sigma value (estimated assuming its independence from the orbit error) are not known. A candidate, among others, is the ocean tide correction error because aliasing frequencies of M_2 and S_2 constituents are intraseasonal frequencies (about 60 days in period) for the T/P altimeter data sampling (Schlax and Chelton, 1994b). The fluctuations, however, are not different between the two ocean tide corrections by the Cartwright and Ray (1991) and Schwiderski (1980) models, and they are not periodic (Fig. 3), which fact suggests that most of the fluctuations are not due to aliasing of the tidal correction error. Aliasing of the ocean tide correction error in the altimeter data processing is discussed in detail by Jacobs *et al*. (1992) and Schlax and Chelton (1994a).

Comparison is generally good for the fluctuation component of SSDT among the altimetry, hydrography and tide gauge measurements (Fig. 6). The altimeter and tide gauge measure the sum of barotropic and baroclinic components of the SSDT, while the hydrographic survey measures only the baroclinic signal and the SSDT estimated from hydrographic data misses the barotropic component. The altimeter and tide gauge data also include non-geostrophic components such as wind drift effect, unsteadiness and nonlinearity, which are important in some cases (e.g., Richardson *et al*., 1992). A rather large discrepancy found in the strongest part of the Kuroshio south of Cape Ashizuri on Pass 112 in case II comparison (see Table 1) may be explained by these differences. It should be noted also that the Prompt Report (Fig. 2) shows a small southward meander appearing off Cape Ashizuri in early June 1993. It may have happened that the hydrographic survey on May 30–31 described the Kuroshio before the appearance of this meander, while the altimeter measurement on June 2 in Cycle 26 described the Kuroshio which was meandering and flowing along the subsatellite track locally; namely, the discrepancy may be due to the time difference between the two measurements, even though the difference is fairly small (2–3 days). It is also possible that a fairly large-amplitude barotropic disturbance was located occasionally off Cape Ashizuri at the time of that altimeter measurement. The coastal tide gauge, however, does not show any significant increase of the sea level at that time, which indicates that the tide gauge happened to miss the signal because it was apart from the possible disturbance, or that the barotropic disturbance did not exist at all. We need direct current measurements in the Kuroshio to detect its barotropic flow field.

The Kuroshio axis was stable south of Cape Shiono-misaki (Pass 188), taking non-large-meander paths during the T/P measurements, and the one year mean SSDT there could, therefore, be much steeper than the climatological mean SSDT, which is an average both for the large-meander and non-large-meander paths, resulting in the broad and weak mean Kuroshio. This fact partially explains the weaker geostrophic velocities estimated near the coast along Pass 188 (Fig. 7d). The situation can be improved when altimeter data for a longer period are available. The next improvement could be making the mean fields both for large-meander and non-large-meander periods and using either mean field as the mean field over the observation period if either one condition persists during the analysis period.

One may want to adjust the mean SSDT field by adding the difference between a single instantaneous hydrographic SSDT profile (or an average of several profiles) and the composite SSDT, but this may not necessarily provide us with a more accurate mean SSDT because a considerable amount of discrepancy may exist occasionally between the altimetric and hydrographic measurements as is shown in Fig. 6. Careful and detailed examination is needed.

The comparison (Fig. 5) of the composite SSDT with the hydrographic SSDT is probably not much affected by the uncertainty associated with the large-scale intraseasonal fluctuations of unknown origin shown in Fig. 3. Arrows for Pass 112 in Fig. 3 show cycles for which the comparison is made. Fortunately, every comparison happens to have been made when the large-scale fluctuation SSDT was very close (within 5 cm) to the level of the annual cycle and the comparison shown in Fig. 5 is, therefore, probably not much affected by this uncertainty.

The comparison of locations of estimated strong eastward geostrophic velocities with reported locations of the Kuroshio axis is very good for Passes 36, 10 and 86 (Figs. 7b, e and f), where the Kuroshio path fluctuated extensively, while it is not very good for Passes 112 and 188 (Figs. 7c and d), where the path was stable, as was expected in the Introduction. It suggests that the fluctuation component is estimated fairly well by the altimeter, but the mean field used for composite SSDT may not be accurate enough. In the latter case (Passes 112 and 188), no large geostrophic velocities are estimated near the coast during several cycles even though the Kuroshio axis is reported there by the Prompt Report. This could be because the actual geostrophic velocity during those cycles was close to the one year mean geostrophic velocity, which may have been approximated lower than it actually was, with the present climatological mean. Table 4 shows that the fluctuation of locations of the maximum estimated geostrophic velocity compares well statistically with the fluctuation of locations of the Kuroshio axis shown in the Prompt Report, except for Pass 203. This is probably because the fluctuation of locations of the maximum estimated velocity is determined mostly by the temporal fluctuation component estimated fairly accurately by the altimeter.

The amplitude of the estimated geostrophic velocities is probably underestimated, especially where the Kuroshio path was stable, but there are no appropriate data to compare with. There are no suitable data, either, to compare with the geostrophic velocity profiles in details. One exception is a data set of surface velocities measured repeatedly by an acoustic Doppler current profiler mounted on a ferry boat crossing the Kuroshio between T/P descending passes 10 and 86 (Ebuchi and Hanawa, 1995); a favorable comparison is found between fluctuation part of the altimeter-derived geostrophic velocities and that of those *in situ* surface velocities.

The situation of the composite SSDT near the coast is also made worse by the fact that the water depth there is less than 1,000 m and climatological mean sea surface geopotential anomalies referred to 1,000 dbar surface cannot be estimated properly; we are forced to extrapolate the values to the coast. This may explain the rather poor comparison of the Kuroshio for Pass 203 (Fig. 7a) at the Tokara Strait. We tried to estimate geostrophic velocities for the Kuroshio in the East China Sea by the same method, but the results were worse. This is probably because the Kuroshio path was stable there and more accurate one year mean SSDT is required and partly because the Kuroshio is usually located on the continental slope (shallower than 1,000 m) in the East China Sea (Yamashiro *et al.* 1990; Ichikawa and Beardsley, 1993) and geopotential anomalies referred to 1,000 dbar surface miss the strongest part of the flow. The weaker mean field is partly due to the coarse resolution of the present climatological mean SSDT field of a $1° \times 1°$ grid.

The present climatological mean SSDT does not include the barotropic component of SSDT;

namely, the reference velocity at 1,000 dbar surface is ignored, because velocities of deep layers in the Kuroshio south of Japan are not known satisfactorily. Velocities near the bottom under the Kuroshio were measured by moored current meters at several stations for 1–3 months, showing that the flow field is very variable and also that geostrophic velocities referred to the observed velocities indicate a narrow deep flow coherent with the surface Kuroshio as well as a deep countercurrent on the continental slope (Taft, 1978). On the other hand, moored current meter measurements south of Kyushu showed the eastward flowing Kuroshio was confined to the upper 600 m in 1–5 month averages (Takematsu *et al.*, 1986). We need more detailed velocity observations for the deep Kuroshio to obtain reliable reference velocities at a deep layer.

Since October 1993, affiliated intensive oceanographic surveys of the Kuroshio and Kuroshio Countercurrent off Shikoku have been under way along the T/P subsatellite Pass 112. An extensive array of moored current meters and other instruments has been maintained along the pass, and CTD/XBT measurements are being made as frequently as possible during the two year observation period. Those data can be combined to give numbers of *in situ* absolute (namely, barotropic plus baroclinic) SSDT profiles under assumption of geostrophy. From those absolute SSDT profiles and fluctuation SSDT derived from T/P altimetry data, we can estimate the mean SSDT during the altimetry mission fairly accurately, and then a time series of absolute SSDT will be obtained.

Another effort to detect oceanic flows including the stable Kuroshio is the improvement of the geoid model with ship gravity measurements, even if the surveys may be limited to local areas (Fukuda, 1990; Zlotnicki and Marsh, 1989). The geoid model thus improved can be assessed by examining the absolute SSDT derived from combined use of this geoid model and altimetry data (e.g, Ichikawa and Imawaki, 1996).

5. Summary

The T/P altimeter data from the first 38 repeat cycles (one year) are used to detect the fluctuation component of SSDT for the Kuroshio region south of Japan. The detected fluctuation SSDT is combined with a climatological mean SSDT to provide us with a composite SSDT which is intended to be an approximation of the total SSDT.

The fluctuation component of SSDT averaged over a wider area in the western North Pacific (mostly in the Philippine Basin) shows a clear annual cycle with an amplitude of about 15 cm, which is probably due to the heating and cooling of the surface layer. Also found are large-scale (longer than 1,500 km) intraseasonal fluctuations of about 9 cm rms magnitude. Some of the fluctuation (4 cm) may be the real sea level rising and falling over the whole area and some (4 cm) is probably due to the orbit error (Fu *et al*., 1994), but the error sources of the remaining fluctuation (7 cm) are not known.

Temporal changes of SSDT determined from altimeter measurements in the Kuroshio region compare moderately well with temporal changes of baroclinic SSDT estimated from repeated hydrographic measurements along a subsatellite track, although there are some discrepancies of unknown origin. They compare well with temporal changes of the sea level at a tide gauge station near the track. The composite SSDT also compares well with the SSDT estimated from the same hydrographic data. Horizontal distribution of the surface geostrophic velocity component normal to subsatellite tracks is derived from the composite SSDT every ten days. Most locations of estimated strong eastward geostrophic velocities coincide well with locations of the Kuroshio axis shown in the Prompt Report, which were determined every 15 days principally from *in situ* surface velocities measured with acoustic Doppler current meters on

various vessels. Steady northeastward propagation of a meander of the Kuroshio is clearly detected southeast of Kyushu, having a meridional phase speed of about 3 cm/sec, in the time series of the estimated surface geostrophic velocities. The disturbance developed to be a fairly large meander of the Kuroshio south of Honshu. An associated recirculation in the shore-side cyclonic cold water mass region is also observed in these time series.

In conclusion, the composite SSDT derived from altimeter data and the climatological mean SSDT can detect fluctuations of the Kuroshio axis moderately well.

Acknowledgements

We thank Kaoru Ichikawa and Hiroshi Uchida for helping us with data processing, and Mark Wimbush for reading the original manuscript very carefully. We also thank Hiroshi Kawamura, Richard Coleman and anonymous reviewers for their valuable comments. The cooperation of the captains and crew of the R/V Shoyo of the Hydrographic Department, R/V Shumpu-maru of Kobe Marine Observatory and R/V Kaiyo of Japan Marine Science and Technology Center is appreciated. The T/P altimeter data were provided by the Physical Oceanography Distributed Active Archive Center at the Jet Propulsion Laboratory/California Institute of Technology. The climatological mean geopotential anomalies at the sea surface were provided by the Japan Oceanographic Data Center. Reports entitled “Prompt Report on Oceanographic Conditions”, issued semimonthly by the Hydrographic Department were very useful for the present study. This study is a part of the activities of the NASA-approved Japanese T/P science group for physical oceanography. This research was supported in part by a Grant-in-Aid for Scientific Research and an International Cooperative Research Project, GOOS (Global Ocean Observing System), both from the Ministry of Education, Science and Culture, and also by the Science and Technology Agency, Japan.

References

Aoki, S., S. Imawaki and K. Ichikawa (1995): Baroclinic disturbances propagating westward in the Kuroshio Extension region as seen by a satellite altimeter and radiometers. *J. Geophys. Res*., **100**(C1), 839–855.

AVISO (1992): AVISO User Handbook: Merged TOPEX/POSEIDON Products, *AVI-NT-02-101-CN*, Edition 1.

Callahan, P. S. (1993): TOPEX/POSEIDON Project GDR Users Handbook, *Jet Propulsion Laboratory D-8944*.

Cartwright, D. E. and R. D. Ray (1991): Energetics of global ocean tides from Geosat altimetry. *J. Geophys. Res*., **96**(C9), 16,897–16,912.

Cheney, R. E., B. C. Douglas and L. Miller (1989): Evaluation of Geosat altimeter data with application to tropical Pacific sea level variability. *J. Geophys. Res*., **94**(C4), 4737–4747.

Cheney, R. E. and J. G. Marsh (1981): Seasat altimeter observations of dynamic topography in the Gulf Stream region. *J. Geophys. Res*., **86**(C1), 473–483.

Cheney, R. E., J. G. Marsh and B. D. Beckley (1983): Global mesoscale variability from collinear tracks of SEASAT altimeter data. *J. Geophys. Res*., **88**(C7), 4343–4354.

Douglas, B. C., D. C. McAdoo and R. E. Cheney (1987): Oceanographic and geophysical applications of satellite altimetry. *Rev. Geophys*., **25**, 875–880.

Ebuchi, N. and K. Hanawa (1995): Comparison of surface current variations observed by TOPEX altimeter with TOLEX-ADCP data. *J. Oceanogr*., **51**, 351–362.

Fu, L.-L. (1983): Recent progress in the application of satellite altimetry to observing the mesoscale variability and general circulation of the oceans. *Rev. Geophys. Space Phys*., **25**, 1657–1666.

Fu, L.-L, E. J. Christensen, C. A. Yamarone, Jr., M. Lefebvre, Y. Menard, M. Dorrer and P. Escudier (1994): TOPEX/POSEIDON mission overview. *J. Geophys. Res*., **99**(C12), 24,369–24,381.

Fukasawa, M. and T. Teramoto (1986): Characteristics of deep currents off Cape Shiono-misaki before and after formation of the large meander of the Kuroshio in 1981. *J. Oceanogr. Soc. Japan*, **42**, 53–68.

Fukuda, Y. (1990): Precise determination of local gravity field using both the satellite altimeter data and the surface gravity data. *Bull. Ocean Res. Inst., Univ. Tokyo*, **28**, 133 pp.

Glenn, S. M., D. L. Porter and A. R. Robinson (1991): A synthetic geoid validation of Geosat mesoscale dynamic topography in the Gulf Stream region. *J. Geophys. Res*., **96**(C4), 7145–7166.

Horton, C. W., D. L. Porter, P. W. deWitt and W. E. Rankin (1992): Airborne expendable bathythermograph survey of the Kuroshio Extension and comparison with simultaneous altimeter measurements during the Geosat Exact Repeat Mission. *J. Geophys. Res*., **97**(C5), 7447–7463.

Gaspar, P., P. Ogor, P.-Y. Le Traon and O.-Z. Zanife (1994): Estimating the sea state bias of the TOPEX and POSEIDON altimeters from crossover differences. *J. Geophys. Res*., **99**(C12), 24,981–24,994.

Ichikawa, H. and R. C. Beardsley (1993): Temporal and spatial variability of volume transport of the Kuroshio in the East China Sea. *Deep-Sea Res*., **40**, 583–605.

Ichikawa, K. and S. Imawaki (1994): Life history of a cyclonic ring detached from the Kuroshio Extension as seen by the Geosat altimeter. *J. Geophys. Res*., **99**(C8), 15,953–15,966.

Ichikawa, K. and S. Imawaki (1996): Estimating the sea surface dynamic topography from Geosat altimetry data. *J. Oceanogr*., **52** (in press).

Ichikawa, K., S. Imawaki and H. Ishii (1995): Comparison of surface velocities determined from altimeter and drifting buoy data. *J. Oceanogr*., **51**, 729–740.

Imawaki, S. and K. Ichikawa (1991): Fluctuation of the Kuroshio Extension as seen by a satellite altimeter. *Umi to Sora*, **67**, 133–151 (in Japanese with English abstract).

Imawaki, S., K. Ichikawa and H. Nishigaki (1991): Mapping the mean sea surface elevation field from satellite altimetry data using optimal interpolation. *Marine Geodesy*, **15**, 31–46.

Jacobs, G. A., G. H. Born, M. E. Parke and P. C. Allen (1992): The global structure of the annual and semiannual sea surface height variability from Geosat altimeter data. *J. Geophys. Res*., **97**(C11), 17,813–17,828.

Kawabe, M. (1985): Sea level variations at the Izu Islands and typical stable paths of the Kuroshio. *J. Oceanogr. Soc. Japan*, **41**, 307–326.

Kawai, H. (1969): Statistical estimation of isotherms indicative of the Kuroshio axis. *Deep-Sea Res*., **16**, 109–115.

Kelly, K. A. and S. T. Gille (1990): Gulf Stream surface transport and statistics at 69°W from the Geosat altimeter. *J. Geophys. Res*., **95**(C3), 3149–3161.

Nerem, R. S., B. D. Tapley and C. K. Shum (1990): Determination of the ocean circulation using Geosat altimetry. *J. Geophys. Res*., **95**(C3), 3163–3179.

Masuzawa, J. (1969): Note on characteristics of the strongest part of the Kuroshio. *J. Oceanogr. Soc. Japan*, **25**, 259–260.

Mitchum, G. T. (1994): Comparison of TOPEX sea surface heights and tide gauge sea levels. *J. Geophys. Res.*, **99**(C12), 24,541–24,553.

Picaut, J., A. J. Busalacchi, M. J. McPhaden and B. Camusat (1990): Validation of the geostrophic method for estimating zonal currents at the equator from Geosat altimeter data. *J. Geophys. Res*., **95**(C3), 3015–3024.

Qiu, B. (1992): Recirculation and seasonal change of the Kuroshio from altimetry observations. *J. Geophys. Res*., **97**(C11), 17,801–17,811.

Qiu, B. (1994): Determining the mean Gulf Stream and its recirculations through combining hydrographic and altimetric data. *J. Geophys. Res*., **99**(C1), 951–962.

Qiu, B., K. A. Kelly and T. M. Joyce (1991): Mean flow and variability of the Kuroshio Extension from Geosat altimetry data. *J. Geophys. Res*., **96**(C10), 18,491–18,507.

Richardson, P. L., S. Arnault, S. Garzoli and J. G. Bruce (1992): Annual cycle of the Atlantic North Equatorial Countercurrent. *Deep-Sea Res*., **39**, 997–1014.

Schlax, M. G. and D. B. Chelton (1994a): Detecting aliased tidal errors in altimeter height measurements. *J. Geophys. Res*., **99**(C6), 12,603–12,612.

Schlax, M. G. and D. B. Chelton (1994b): Aliased tidal errors in TOPEX/POSEIDON sea surface height data. *J. Geophys. Res*., **99**(C12), 24,761–24,775.

Schwiderski, E. W. (1980): On charting global ocean tides. *Rev. Geophys. Space Phys*., **18**, 243–268.

Taft, B. (1972): Characteristics of the flow of the Kuroshio south of Japan. p. 165–216. In *Kuroshio—Its Physical Aspects*, ed. by H. Stommel and K. Yoshida, University of Tokyo Press, Tokyo.

Taft, B. A. (1978): Structure of Kuroshio south of Japan. *J. Mar. Res*., **36**, 77–117.

Tai, C.-K. (1990): Estimating the surface transport of meandering oceanic jet streams from satellite altimetry: Surface transport estimates for the Gulf Stream and Kuroshio Extension. *J. Phys. Oceanogr*., **20**, 1761–1777.

Taira, K. and T. Teramoto (1981): Velocity fluctuations of the Kuroshio near the Izu Ridge and their relationship to current path. *Deep-Sea Res*., **28**, 1187–1197.

Takano, I., S. Imawaki and H. Kunishi (1981): TS dynamic height calculation in the Kuroshio region. *La mer*, **19**, 75–84.

Takematsu, M., K. Kawatate, W. Koterayama, T. Suhara and H. Mitsuyasu (1986): Moored instrument observations in the Kuroshio south of Kyushu. *J. Oceanogr. Soc. Japan*, **42**, 201–211.

Willebrand, J., R. H. Käse, D. Stammer, H.-H. Ninrichsen and W. Krauss (1990): Verification of Geosat sea surface topography in the Gulf Stream extension with surface drifting buoys and hydrographic measurements. *J. Geophys. Res*., **95**(C3), 3007–3014.

Wyrtki, K. (1975): Fluctuations of the dynamic topography in the Pacific Ocean. *J. Phys. Oceanogr*., **5**, 450–459.

Yamashiro, T., A. Maeda, M. Sakurai and H. Ichikawa (1990): Mean velocity distribution and transport of the Kuroshio referred to GEK surface velocity in the East China Sea. *Umi to Sora*, **66**, 181–190 (in Japanese with English abstract).

Zlotnicki, V. and J. G. Marsh (1989): Altimetry, ship gravimetry, and the general circulation of the North Atlantic. *Geophys. Res. Lett*., **16**, 1011–1014.